

Vapor contribution to the time dependence of the effective diffusion coefficient in partially filled porous glasses

Germán Farrher¹, Ioan Ardelean^{2,}, Rainer Kimmich¹*

¹ University of Ulm, Sektion Kernresonanzspektroskopie, 89069 Ulm, Germany

² Technical University of Cluj Napoca, Physics Department, 400020 Cluj-Napoca, Romania

Corresponding author: Ioan Ardelean, Technical University of Cluj Napoca, Physics Department, 400020 Cluj-Napoca, Romania, E-Mail: ioan.ardelean@phys.utcluj.ro

(received 12 June 2007, accepted 3 July 2007)

Abstract

NMR microscopy of silica glasses with micrometer pores (Vitrapor#5) partially filled with water reveal heterogeneous distributions of the liquid on a length scale much longer than the pore dimension. This heterogeneity, which is not observed in MRI of saturated samples, is attributed to the spatial variation of the granular microstructure. As a consequence of the inhomogeneous filling degree, the effective transverse relaxation time varies, which in turn leads to NMR imaging contrasts. Since the spatial distribution of the transverse relaxation time prevents reliable measurements with the standard pulsed gradient stimulated echo technique (PGStE), a combination of the fringe field stimulated echo method (FFStE) on the one hand and the magnetization grid rotating frame imaging technique (MAGROFI) on the other was employed in our investigations. Using this combination four decades of the diffusion time from 100 μ s to 1 s could be probed. The comparison of the experimental data with Monte Carlo simulations on a model structure has shown that the vapor phase contribution to the effective diffusivity is particularly efficient on a diffusion time scale corresponding to root mean squared displacements of the order of pores dimension.

Keywords

NMR, diffusion, partially filled, porous media, vapor phase

1. Introduction

Unsaturated porous media are systems of coexisting liquid and vapor phases subject to geometrical restrictions by a pore network, molecular exchange, and adsorption-desorption processes. The consequence is that the effective diffusion coefficient tends to be a function of the diffusion time t . A time dependent diffusion coefficient is defined by [1]

$$D(t) = \langle r^2(t) \rangle / 6t, \quad (1)$$

where $\langle r^2(t) \rangle$ is the mean squared displacement of molecules. The time dependence is of particular interest because it globally reflects the spatial distribution of the liquid in the pore space, the molecular exchange rates, the polarity of the liquid and the pore walls, and the geometrical character of the confining pore space.

Porous silica glasses are random objects intrinsically implying spatially fluctuating heterogeneities of the local pore size, the local magnetic susceptibility, the local transverse relaxation time of the fluid, the local diffusion coefficient and other properties. These heterogeneities can be characterized by introducing spatial correlation functions of given correlation lengths that may vary in an extremely wide range depending on the material. It will be shown here that the porous glass, VitraPor#5, with a nominal pore size of about 1 μm is subject to heterogeneities almost approaching the sample size. The use of a porous glass with pores in the μm regime thus permits one to explore the nature of the heterogeneities and their influence on measuring quantities such as the diffusion coefficient.

Transverse relaxation in unsaturated porous glasses is expected to be largely inhomogeneous as a consequence of the spatially varying filling degree. Anticipating that the relaxation rates are weighted by the fraction of molecules in the adsorption layer at the solid/liquid interfaces, one concludes that a locally large filling degree leads to long relaxation times whereas surfaces just covered by a thin liquid layer with no surrounding bulklike water will produce short relaxation times. Both situations occur in partially filled pore spaces. That is why, any NMR technique for measuring diffusion coefficients should be particularly insensitive to spatial variations of the transverse relaxation time T_2 . In the present work a combination of the fringe field stimulated echo method (FFStE) [2,3] on the one hand and the magnetization grid rotating frame imaging technique (MAGROFI) [4,5] on the other was employed. Using this combination four decades of the diffusion time from 100 μs to 1 s could be probed [6].

There is a number of models for the spatial fluid distribution in partially filled porous media [7,8]. These morphology models often refer to structure units such as plugs, puddles, surface layers of constant thickness, etc., which seem to be of a somewhat artificial character. In the present study, we therefore try to model the spatial distribution of the fluid in a more natural way: Assuming a granular type of the porous matrix (as it occurs in typical porous silica glasses) and considering more or less overlapping liquid surface layers produces structure elements such as plugs, interface layers of varying thickness, and droplet-like accumulations of the liquid phase “automatically”. Monte Carlo simulations of molecular diffusion in this sort of model system will be the main tools for the interpretation of the experimental NMR results.

2. Experimental

2.1. Sample preparation and characterization

The sample under investigation is a silica glass, VitraPor#5, with pores in the mesoscopic range (nominal pore size 1 $\mu\text{m} \pm 0.6 \mu\text{m}$; porosity 0.43). It was purchased from ROBU Glasfilter-Geräte GmbH, Germany. The sample was pretreated as suggested by the manufacturer. This includes 30 minutes of boiling in 30 % H_2O_2 . The sample was then washed

with distilled water and left in vacuum for 24 hours at 95 °C. After that, the sample was considered to be dry. That is, the nominal filling factor was set $f = 0$ under such conditions.

The adsorbate fluid was demineralised water. It was filled into the porous glass either via *adsorption* (the dry material was placed in a saturated atmosphere until the desired filling factor was reached) or via *desorption* (the saturated material was exposed to a dry atmosphere until the desired degree of filling was established). In either case the filling factor was determined by weighing. In the “adsorption mode” (AM), the adsorbate was heated to 60 °C in order to increase the vapor pressure and hence to accelerate the uptake of the adsorbate in the porous material. In the “desorption mode” (DM), the sample was first saturated with the aid of the bulk-to-bulk method resulting in a filling factor 1. Afterwards the liquid in the pores was partially evaporated by putting the sample in a glove bag with a dry nitrogen atmosphere. In this way, any contact with the humidity of the air was avoided. After preparation, the sample was sealed in a sample container with practically no empty space that would allow for further evaporation. Extended annealing of the samples did not perceptibly affect the heterogeneous distribution of the liquid in the sample (see below).

NMR micrographs were recorded using the standard two-dimensional (2DFT) Fourier transform imaging technique, which is based on Hahn echo pulse sequences (see refs. [1] or [9] for details). Cross sectional images are rendered in Fig. 1. All parameters of the sample preparation and of the image acquisition are given in the legends or are specified directly in the images. The experiments were performed at 20°C on a Bruker DSX 400MHz NMR spectrometer equipped with a microscopy gradient unit. The maximum strength of gradient pulses achievable with this instrument both for imaging and diffusometry was 1 T/m.

Figure 1a shows a cross-sectional NMR image of a VitraPor#5 sample saturated with water ($f = 1$). Apart from noise, no contrast inside the sample can be identified. That is, the voxel-average water spin density and the voxel-average transverse and longitudinal relaxation times do not vary from voxel to voxel where the voxel dimension is much larger than the nominal pore size.

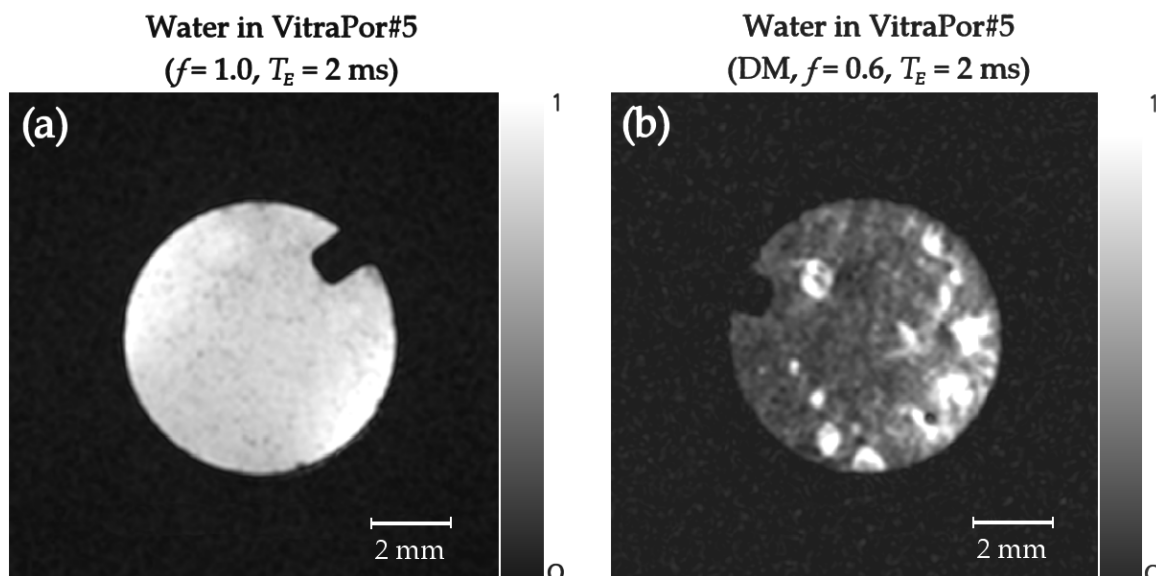


Fig. 1: NMR micrographs of water in saturated (a) and unsaturated (b) VitraPor#5 porous silica glass. The echo time (T_E), the filling degree (f), and the preparation method (DM = desorption mode) are indicated in the images. The repetition time was $T_R = 1$ s in both cases. The cross section is directly measured with the aid of a two-dimensional slice selective imaging sequence (2DFT; slice width 1 mm).

The situation is quite different in the case of unsaturated sample. Figure 1b shows a cross-sectional NMR micrograph of VitraPor#5 samples with a filling degree $f = 0.6$. One can observe there light spots indicating a high content of the liquid phase. The preparation technique of the sample in Fig. 1 was the desorption mode (DM) but the way how the samples is filled appears to be of relatively little influence on the spatial distribution. Irrespective of whether desorption or adsorption mode was used, the heterogeneous distribution of the liquid phase turns out to be rather similar.

One might think of a metastable distribution of the liquid phase fortuitously arising due to some imponderabilities in the preparation procedure. However, even extended annealing periods (up to weeks) of the sealed samples at elevated temperatures (up to 90°C) did not change the coarse grain distribution of the liquid phase. It appears that the spatial distribution does not depend on the preparation history. It can also not be solely due to instability between the vapor and liquid phases as a consequence of the competition between cohesion and adhesion forces. This would stipulate much more variability in the morphology of the spatial phase distribution than observed. The conclusion is that the heterogeneity has a microstructural origin. Actually electron micrographs (not shown here) suggest this sort of heterogeneity.

In Fig. 1 the NMR images are strongly weighted by relaxation. In particular, liquid in the light spots tends to have a longer T_2 than in the darker areas. An explanation is that the higher filling degree in the light spots produces a more homogeneous filling and, hence, less susceptibility fluctuations. It is often assumed that the correlation length of a porous medium is of the order of a few pore diameters. However, the fact that it was possible to visualize microscopic heterogeneities in the structure of the VitraPor#5 sample partially filled with liquids indicates much longer correlation lengths.

2.2. Diffusion techniques

As suggested in a previous study [6], a particularly favorable combination of NMR diffusometry methods for time dependent diffusion studies is the fringe field stimulated echo (FFStE) technique [2,3] for relatively short diffusion times ($100 \mu\text{s} < t < 10 \text{ ms}$), and the magnetization grid rotating frame imaging (MAGROFI) variant [4,5] for long diffusion times ($10 \text{ ms} < t < 1 \text{ s}$). The former is insensitive to internal gradients due to the large external field gradient employed (up to 60 T/m on our spectrometer), the latter because of the use of gradients of the radio frequency amplitude, which is practically not affected by inhomogeneities of the magnetic susceptibility. Owing to the extremely short coherence evolution intervals of the FFStE method and the fact that the MAGROFI technique is essentially based on the evolution of the longitudinal magnetization, ensure that transverse relaxation in general and distributions of the local T_2 in particular are of negligible influence.

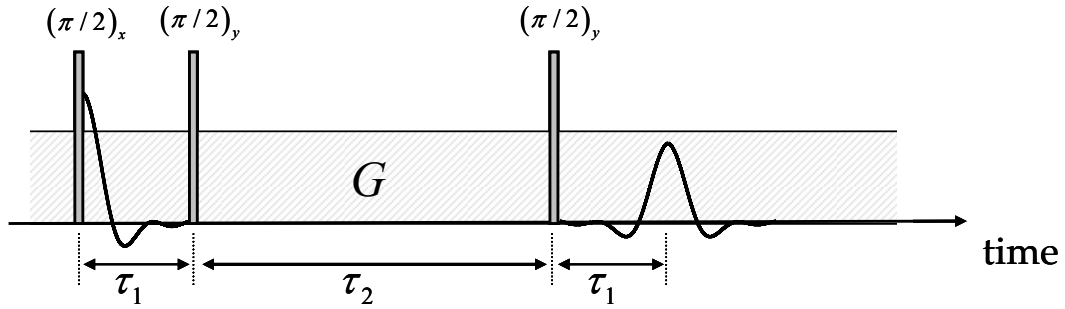
Figure 2 shows the pulse schemes for the NMR diffusometry experiments in this study. The fringe-field stimulated echo pulse sequence (Fig.2a) consists of three radio frequency (RF) pulses. The spin coherences evolve in the presence of the steady external gradient G of the fringe field of the superconducting magnet. In the present experiments, the field gradient was chosen to be $G = 22 \text{ T/m}$ at a position 15.6 cm below the center of the magnet. The probe for the FFStE experiments was tuned to 375 MHz at a field gradient of 22 T/m. The magnetic flux density and its gradient were first crudely measured with the aid of a homemade Hall probe. The gradient was then calibrated with the known diffusion coefficient of bulk water.

The attenuation factor of the stimulated echo following the third RF pulse is given by [1]

$$A = A_0 e^{-D\gamma^2 G^2 \tau_1^2 (\frac{2}{3}\tau_1 + \tau_2)} e^{-\frac{2\tau_1}{T_2}} e^{-\frac{\tau_2}{T_1}}, \quad (2)$$

where D is the diffusion coefficient, γ is gyromagnetic ratio and T_1 and T_2 are the longitudinal and transverse relaxation times, respectively. Note that diffusive displacements during the

a) FFStE



b) MAGROFI

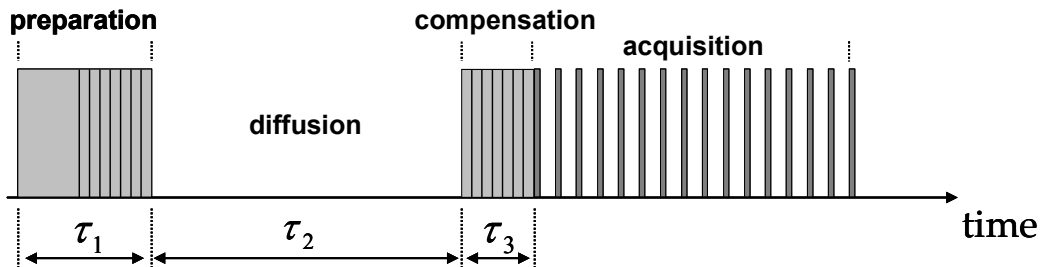


Fig. 2: a) Schematic representation of the radio frequency (RF) pulses and the steady field gradient for the fringe field stimulated-echo variant of NMR diffusometry (FFStE). In the present study, a steady gradient $G = 22 \text{ T/m}$ is applied along the z -axis. The time τ_1 is varied from $10 \mu\text{s}$ to $106 \mu\text{s}$ in 32 steps. b) RF gradient pulse scheme of the MAGROFI experiment as used in the present study. The preparation pulse is incremented in subsequent transients from a starting value of $180 \mu\text{s}$ in 32 steps of $\tau_r = 20 \mu\text{s}$ each. The magnetization grid produced by the preparation pulse is recorded after the diffusing interval by a rapid rotating frame imaging technique. The compensation pulse effectively stretches the magnetization grid to be imaged so that the wavelength of the modulation remains constant independent of the preparation pulse length.

interval τ_1 (see Fig. 1a) can be neglected as long as the condition $\tau_1 \ll \tau_2$ is fulfilled, so that the diffusion time can be equated with τ_2 . On the other hand, if the τ_2 interval is comparable with τ_1 , the diffusion time can be defined by $t_{diff} \equiv \frac{2}{3}\tau_1 + \tau_2$ which is to be kept constant in an experiment (see Ref. [6]).

The time interval τ_1 was varied from $10 \mu\text{s}$ to $106 \mu\text{s}$ in 32 steps. Due to the fringe field gradient, T_2^* was extremely short ($\approx 1.2 \mu\text{s}$). That is, diffusion times as short as $100 \mu\text{s}$ could be reached easily, and the FFStE diffusion time window covers the range $100 \mu\text{s}$ to 10 ms . The influence of transverse and longitudinal relaxation was eliminated by repeating exactly the same pulse experiment in a homogeneous field of practically the same strength. Division of the stimulated echo amplitudes with and without field gradient then provides the echo attenuation factor due to diffusion alone. Alternatively self-compensating pulse sequences can be employed as reported in Ref. [10].

The principle of the MAGROFI method is schematically shown in Fig.2b. The technique is based on gradients of the RF amplitude [11]. In order to produce favorable B_1 gradients for the MAGROFI experiments, the RF coil of an ordinary probehead of the system was replaced by a conic coil [6]. Note that the same coil was used for detection and rotating frame imaging.

In the preparation interval, a magnetization grid (or grating) is prepared. A diffusion interval follows. After compensation of the evolution due to the increments of the preparation

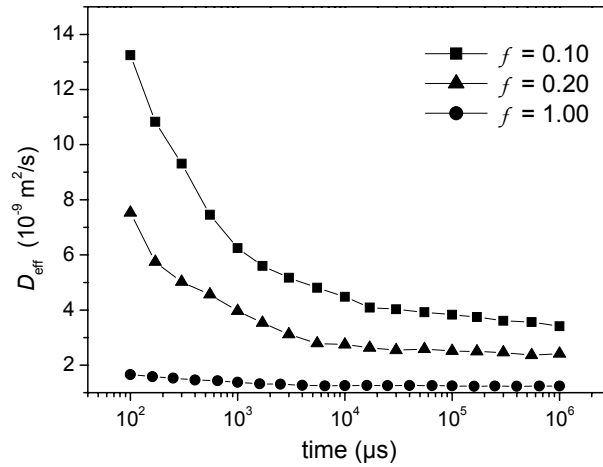


Fig. 3: Effective (= overall average) diffusion coefficient versus diffusion time for different filling factors. The data were measured by a combination of FFStE and MAGROFI techniques.

interval, the longitudinal magnetization distribution is imaged using a rapid rotating frame imaging technique. The width of the preparation and compensation pulses was synchronously incremented in 32 steps of 30 μs each. The initial duration of the preparation pulse was 180 μs. After the interval τ_3 (see Fig. 2b), one-dimensional rapid rotating frame images were rendered by acquiring the pseudo free-induction decay (FID) with a train of 200 pulses, each of 2 μs duration followed by stroboscopic acquisition of the signals between the pulses.

The Fourier transform of this pseudo FID provides an image of the z -magnetization that is attenuated by relaxation and diffusion phenomena. The diffusion coefficient is evaluated according to[6]

$$A(x, \tau_1) = A_0 \cos[\gamma B_1(x)\tau_1] e^{-D[\gamma G_1(x)]^2 \tau_1^2 \tau_2} e^{-\frac{\tau_2}{T_1}}. \quad (3)$$

Here $B_1(x)$ is the local amplitude of the RF field and $G_1(x) = \partial B_1(x) / \partial x$ the corresponding gradient. These quantities were evaluated as described in Ref.[6]. In Eq.(3), diffusive displacements during the preparation and imaging intervals (see Fig. 2b) have been neglected. Otherwise, formalism analogous to the Stejskal/Tanner treatment [12] for finite field gradient pulses must be employed. In the case of our samples, the total time window accessible by the MAGROFI technique ranges from 10 ms to 1 s. Note that Eq. (3) does not depend on the transverse relaxation time T_2 . That is, MAGROFI diffusometry is not only insensitive to internal field gradients but also to transverse relaxation. More detailed descriptions and discussions can be found in refs. [4-6].

3. Experimental results and the comparison with simulations

Due to heterogeneity influence described above the time dependent diffusion measurements were performed using FFStE and MAGROFI technique. The effective water diffusion coefficient was measured in VitraPor#5 with different filling degrees. The data are plotted in Fig. 3 for diffusion times between 100 μs and 1 s. As far as investigated in this study, the values decrease with increasing filling factor as a consequence of the decreasing vapor phase contribution [13-20]. The time dependence of the diffusion coefficient of water in partially filled porous glass also reflects the obstruction by the pore space tortuosity.

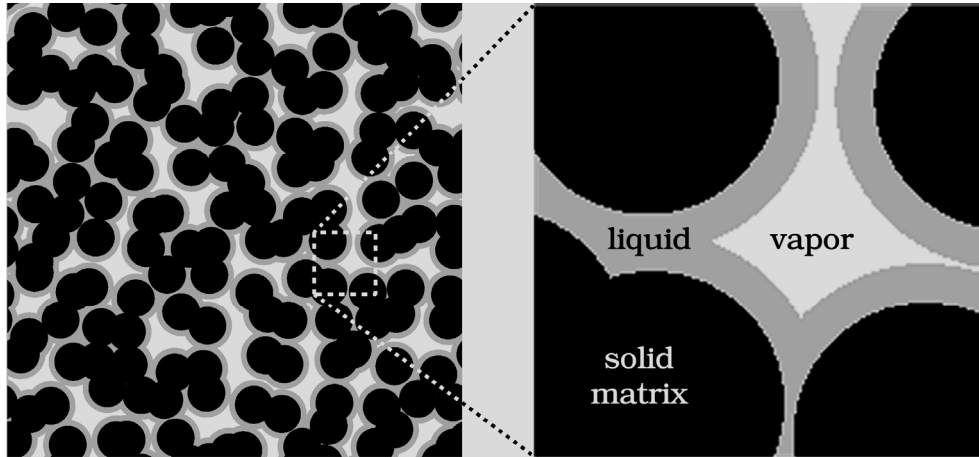


Fig. 4: Spherical-grain pack structure to which refer the Monte Carlo simulations. The solid grains are represented in black, the liquid phase in gray, and the vapor phase in white.

In order to understand the experimental data, Monte Carlo simulations of translational diffusion were performed for two-dimensional model pore spaces (see Fig. 4). Up to 100,000,000 molecular steps of a length corresponding to 1 nm and 100 nm in the liquid and vapor phases, respectively, were simulated using the random number generator routine *ran3* described in ref. [21]. The difference of two orders of magnitude in the step length between the two phases corresponds to four orders of magnitude larger diffusion coefficients known for gases relative to liquids.

The number of fluid molecules considered in the simulation was varied for different diffusion times. For very short times beginning with 125 ps, 10,000,000 particles were necessary to obtain the same statistical accuracy as for long times up to 12.5 ms, where only 1,000 particles were sufficient.

The two-dimensional pore space is defined in a plane with orthogonal Cartesian coordinate axes for x and y . For each molecular step, two random numbers x and y were randomly generated between -1 and +1. The step coordinates are then calculated as

$$\Delta x = \frac{x}{\sqrt{x^2 + y^2}}; \quad \Delta y = \frac{y}{\sqrt{x^2 + y^2}}. \quad (4)$$

The step was cancelled if it leaves the predefined pore space. The mean-squared displacement starting from a randomly chosen initial position was determined as a function of time, and the time-dependent diffusion coefficient was evaluated according to Eq. (1).

Since the density of the liquid phase is three orders of magnitude larger than in the vapor phase, practically the whole signal detectable in our NMR experiments originates from the liquid phase. It is therefore sufficient to consider merely those molecules in the simulations that currently reside in the liquid phase (but possibly have been subject to displacements in the vapor phase areas before).

The Monte Carlo simulations were performed for a grain pack structure as shown in Fig. 4. In two dimensions, the solid grains are represented by circular, partially overlapping discs. The diameter of these circular discs corresponds to 1 μm . The discs were placed at random distances from the lattice points of a square lattice with a unit cell dimension 1 μm . The distance vectors from the lattice points to the associated discs were varied randomly with respect to direction and magnitude. The magnitude varied in the range 0 ... 0.4 μm . The mean pore size resulting in this way is 0.97 μm .

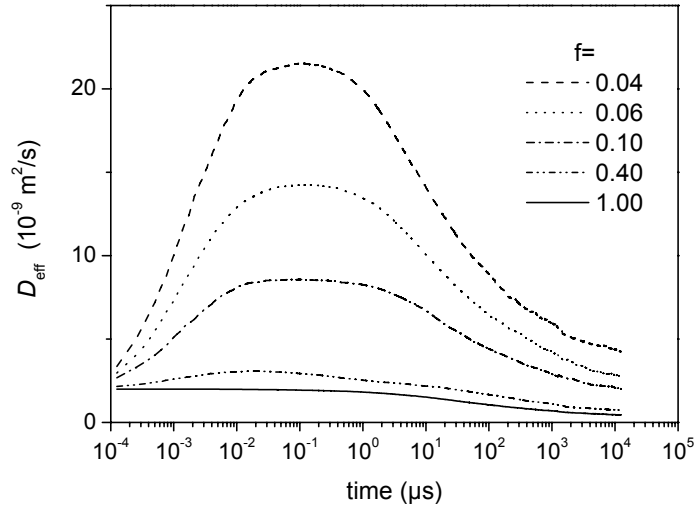


Fig. 5: Effective (= overall average) diffusion coefficient versus diffusion time for different filling factors as obtained from Monte Carlo simulations.

The disc surfaces as far as facing the pore space were assumed to be covered with a liquid layer of constant thickness (see Fig. 4). The remaining pore space represents the vapor phase. When a particle reaches the liquid-vapor interface, the probability per unit time (= step time) to escape from the liquid phase to the vapor phase was assumed to be $P_{l \rightarrow v} = 0.01$. Likewise the probability per unit time that a particle enters the liquid coming from the vapor phase was taken as $P_{v \rightarrow l} = 0.99$. As a third exchange mechanism, adsorption and desorption at the solid matrix walls was considered. The corresponding probabilities per unit time were assumed to be $P_{ads} = 0.9$ and $P_{des} = 0.1$, respectively.

Figure 5 shows the results of Monte Carlo simulations based on the two-dimensional grain model structure rendered in Fig. 4 for different filling factors. As can be observed, the simulations reproduce well the qualitative tendency of the time dependence in the same experimental time window. That means the essential features of pore space restricted diffusion are accounted for. However, the absolute values are significantly different. The reason for the quantitative discrepancies must be sought in the simplicity of the (two-dimensional) model structure in Fig. 4. In particular, the model does not take into account the heterogeneities detected in the microscopy experiments.

4. Conclusions

It is often assumed that the correlation length in a porous media is of the order of a few pore diameters. Here, it was possible to visualize microscopic heterogeneities in the structure of the VitraPor#5 sample partially filled with water. These images are an indication for much longer correlation lengths. The NMR image contrasts are largely dominated by T_2 which strongly varies across the VitraPor#5 samples. This however does not exclude much less heterogeneous distributions of the filling degree and of the local effective diffusion coefficient.

Another finding of our work is that in systems with heterogeneities it is essential to use NMR diffusometry methods insensitive to spatial T_2 distributions. The two techniques employed here (FFStE and MAGROFI) proved to be particularly suitable for time dependent diffusion

studies, in partially filled porous media. These two techniques provide effective diffusion coefficients not affected by spatial variations of the transverse relaxation time.

The last finding of our work is that the diffusion coefficients of liquids in partially filled porous glasses start close to their bulk values in the short time limit corresponding to a few molecular diffusion steps. When the root mean squared displacement approaches the mean pore size, a maximum is reached indicating a significant contribution of the vapor phase to the effective diffusion coefficient via exchange between the two phases (liquid and vapor). Under the present conditions, the maximum value is more than one decade larger than the diffusion coefficient in the bulk liquid. At longer diffusion times (or root mean squared displacement), the obstruction by the tortuosity of the pore space comes into play. The effective diffusion coefficient decays until a reduced effective value close to the bulk liquid value is reached on a length scale beyond the correlation length. The experimental data are reproduced in the common time window by Monte Carlo simulations of a model structure.

Acknowledgments

This work was supported by the Alexander von Humboldt Foundation, the Deutsche Forschungsgemeinschaft, and the Romanian MEC (CNCSIS 1292/2006).

References

- [1] R. Kimmich, *NMR Tomography, Diffusometry, Relaxometry* (Springer-Verlag, Berlin, 1997).
- [2] R. Kimmich and E. Fischer, *J. Magn. Reson. A* **106**, 229 (1994).
- [3] E. Fischer and R. Kimmich, *J. Magn. Reson.* **166**, 273 (2004).
- [4] R. Kimmich, B. Simon, and H. Köstler, *J. Magn. Reson.* **112**, 7 (1995).
- [5] B. Simon, R. Kimmich, and H. Köstler, *J. Magn. Reson. A* **118**, 78 (1996).
- [6] G. Farrher, I. Ardelean, and R. Kimmich, *J. Magn. Reson.* **182**, 215 (2006).
- [7] R. Valiullin, V. Skirda, S. Stapf, and R. Kimmich, *Phys. Rev. E* **55**, 2664 (1997).
- [8] S. G. Allen, P. C. L. Stephenson, and J. H. Strange, *J. Chem. Phys.* **106**, 7802 (1997).
- [9] B. Blümich, *NMR Imaging of Materials* (Clarendon, Oxford, 2000).
- [10] D. E. Demco, A. Johansson, J. Tegenfeldt, *J. Magn. Reson. A* **110**, 183 (1994).
- [11] D. Canet, *Prog. NMR Spectrosc.* **30**, 101 (1997).
- [12] E.O. Stejskal and J.E. Tanner, *J. Chem. Phys.* **42**, 288 (1965).
- [13] I. Ardelean, G. Farrher, C. Mattea, and R. Kimmich, *J. Chem. Phys.* **120**, 9809 (2004).
- [14] J. Kärger, H. Pfeifer, E. Riedel, and H. Winkler, *J. Coll. Interface Sci.* **44**, 187 (1973).
- [15] F. D'Orazio, S. Bhattacharja, W. P. Halperin, and R. Gerhardt, *Phys. Rev. Letters* **63**, 43 (1989).
- [16] R. Kimmich, S. Stapf, P. Callaghan, and A. Coy, *Magn. Reson. Imag.* **12**, 339 (1994).
- [17] R. Kimmich, S. Stapf, R. O. Seitter, P. Callaghan, and E. Khozina, *Mat. Res. Soc. Symp. Proc.* **366**, 189 (1995).
- [18] R. Valiullin, S. Naumov, P. Galvosas, J. Kärger, H.-J. Woo, F. Porcheron, and P. A. Monson, *Nature* **443**, 965 (2006).
- [19] R. Valiullin, P. Kortunov, J. Kärger, and V. Timoshenko, *J. Chem. Phys.* **120**, 11804 (2004).
- [20] I. Ardelean, C. Mattea, G. Farrher, S. Wonorahardjo, and R. Kimmich, *J. Chem. Phys.* **119**, 10358 (2003).
- [21] W. H. Press, B. P. Flannery, S. A. Teukolsky, and W. T. Vetterling, *Numerical Recipes in C* (Cambridge University Press, Cambridge, 1990).